Stereocomplex Formation between Enantiomeric Poly(lactic acid)s. 9. Stereocomplexation from the Melt

Hideto Tsuji† and Yoshito Ikada*,‡

Technology Development Center, Toyohashi University of Technology, 1-1 Tempaku-cho, Toyohashi, Aichi 441, Japan, and Research Center for Biomedical Engineering, Kyoto University, 53 Kawahara-cho, Shogoin, Sakyo-ku, Kyoto 606, Japan

Received May 19, 1993; Revised Manuscript Received August 31, 1993®

ABSTRACT: Stereocomplexation (racemic crystallization) of poly(D-lactic acid) (PDLA) and poly(L-lactic acid) (PLLA) from the melt state was studied using differential scanning calorimetry (DSC) and polarizing microscopy. Complexation predominantly occurred upon annealing the polymer mixtures when the molecular weight of both PDLA and PLLA was below 6×10^3 and the PDLA content (X_D) was between 0.4 and 0.6. In contrast, homocrystallization of PDLA or PLLA prevailed when X_D was around 0 or 1 or the molecular weight of PDLA and PLLA was higher than 1×10^5. The critical molecular weight (M_c) of PDLA and PLLA, below which only racemic crystallites were formed, was lower for the equimolar mixture from the melt than from the solution casting ($M_c = 4 \times 10^4$). The induction period was shorter for racemic crystallization than for homocrystallization. The annealing temperature dependence of the formation of racemic crystalline spherulites was less remarkable than that of the homocrystalline spherulites. When the annealing temperature was lowered from 180 to 80 °C, the average radius of the racemic crystalline spherulites formed at $X_D = 0.5$ decreased from 300 to 50 μm, whereas the average radius of the homocrystalline spherulites of PDLA or PLLA ($X_D = 1$ or 0) dramatically decreased from 2000 to 10 μm.

Introduction

Stereoselective association (stereocomplexation) between optically active polymers, D-polymer and L-polymer, has been reported for various polymer couples; poly(γ-benzyl glutamate),[1–14] poly(γ-methyl glutamate),[15] poly(*tert*-butylthiirane),[16] poly(*tert*-butylethylene oxide),[17] poly(*tert*-butylethylene sulfide),[18] poly(α-methyl-α-ethyl-β-propiolactone) (PMEPL),[19–21] poly(β-(1,1-dichloropropyl)-β-propiolactone),[22] poly(lactic acid) (PLA)[23–32] and its copolymers,[33–35] and poly(α-methylbenzyl methacrylate).[36] These polymers have their chiral carbons in the main chain except for poly(α-methylbenzylmethacrylate), which has the chiral carbons in the side chain. Often, the stereoselective association results in formation of stereocomplex crystallites which are different from the crystallites of the constituent single polymers, D- and L-polymers, in the crystalline structure[1,5,7,16–20,23,30] and melting temperature.[16–20,22,23,36] The crystal structure of stereocomplexes has been reported for poly(γ-benzyl glutamate),[1,5,7] poly(*tert*-butylethylene oxide),[17] poly(*tert*-butylethylene sulfide),[18] and PLA.[30] In these polymers, the stereocomplex crystal is composed of a racemic lattice in which D-polymer and L-polymer or *S*-polymer and *R*-polymer are packed side-by-side in the ratio of 1:1.[1,5,7,17,18,30] We call the stereocomplex crystallite with the racemic lattice the racemic crystallite and the crystallite composed of either D-polymer or L-polymer the homocrystallite.

Since our first report on stereocomplexation (racemic crystallization) between poly(D-lactic acid) (PDLA) and poly(L-lactic acid) (PLLA),[23] we have investigated the stereocomplexation of PDLA and PLLA in terms of various parameters which affect complexation,[23–28] morphology,[27,30,31] phase structure,[29] crystalline structure,[30,31] and degradability.[32] These stereocomplexation studies revealed that stereoselective association between D- and L-polymer occurred preferably to self-association of D- or L-polymer when PDLA and PLLA of low molecular weight were blended at a mixing ratio around 1:1.[23–27] Sphere- or platelet-type particles of PLA stereocomplex having diameter on the order of microns were formed from acetonitrile solutions, their size and shape being affected by various parameters.[27] Electron diffractometry revealed that the platelet-type stereocomplex particle was an assembly of racemic single-crystal lamellas.[27]

Detailed studies were reported on stereocomplexation between optically active enantiomeric polymers from the melt by Prud'homme et al. for (*S*)- and (*R*)-PMEPL,[19,20] but most of the stereocomplexation studies have been performed starting from polymer solutions and little is known about stereocomplexation from the melt state. The present work is concerned with racemic crystallization of PDLA and PLLA from the melt state. Effects of the mixing ratio of the isomers, the molecular weight of the isomers, the annealing time, and the annealing temperature on the thermal properties of the crystallites formed will be studied using differential scanning calorimetry (DSC). The morphology of the assembly of crystallites formed from the melt of blended isomers is also studied with polarizing microscopy.

Experimental Section

Materials. PDLA and PLLA were synthesized with the method previously reported.[37] Methyl D-lactate with an optical purity of 97% was supplied by Daicel Chemical Industries, Ltd., Japan, and hydrolyzed to D-lactic acid. L-Lactic acid with an optical purity of 98% was purchased as a 90 wt % aqueous solution from CCA Biochem BV, The Netherlands. The oligomeric poly(lactic acid)s (PLA) prepared by condensation polymerization of the free acids were thermally decomposed to yield the lactide monomers. Ring-opening polymerization was performed for each lactide in bulk at 140 °C for 10 h using stannous octoate (0.03 wt %) and lauryl alcohol as a polymerization modulator.[38] The polymerization conditions were the same for D- and L-lactides, and the resulting polymers were purified by reprecipitation using methylene chloride as solvent and methanol as precipitant.

The viscosity-average molecular weight ($\bar{M}_v$) of the polymers was determined from their intrinsic solution viscosity [η] in

* To whom correspondence should be addressed.
† Technology Development Center, Toyohashi University of Technology.
‡ Research Center for Biomedical Engineering, Kyoto University.
® Abstract published in *Advance ACS Abstracts*, November 1, 1993.

0024-9297/93/2226-6918$04.00/0

Table I. Polymerization Conditions and Molecular Characteristics of the Polymers

code	polymerization conditions: LA[a] (wt %)	SO[b] (wt %)	temp (°C)	time (h)	molecular characteristics: [η] (dL/g)	$\bar{M}_v$	$[\alpha]^{25}_D$ (deg)
D1	2.5	0.03	140	10	0.30	5.7×10^3	+156
D2	5.0	0.03	140	10	0.36	7.3×10^3	+156
D3	2.0	0.03	140	10	0.61	1.5×10^4	+155
D4	0	0.03	220	5	0.92	2.6×10^4	+154
D5	0.4	0.03	140	10	1.36	4.5×10^4	+156
D6	0	0.03	220	0.5	1.70	6.1×10^4	+154
D7	0	0.03	140	0.3	2.79	1.2×10^5	+156
D8	0	0.03	140	10	7.32	4.5×10^5	+157
L1	3.0	0.03	140	10	0.20	3.3×10^3	−149
L2	2.0	0.03	140	10	0.36	7.3×10^3	−152
L3	1.0	0.03	140	10	0.56	1.3×10^4	−153
L4	0	0.03	140	5	0.96	2.8×10^4	−153
L5	0.5	0.03	140	10	1.30	4.2×10^4	−154
L6	0	0.03	160	5	1.71	6.2×10^4	−151
L7	0	0.03	140	10	3.01	1.3×10^5	−153
L8	0	0.03	140	10	6.98	4.2×10^5	−157

[a] Lauryl alcohol. [b] Stannous octoate.

chloroform at 25 °C using the equation[39]

$$[\eta] = 5.45 \times 10^{-4} \bar{M}_v^{0.73} \quad (1)$$

The specific optical rotation $[\alpha]$ of the polymers was measured in chloroform at a concentration of 1 g/dL and 25 °C using a Perkin-Elmer 241 polarimeter at a wavelength of 589 nm. The characteristics of the polymers used in this work are listed in Table I, together with the polymerization conditions. $[\alpha]^{25}_D$ values were ca. +150° for PDLA and −150° for PLLA, in good agreement with the literature values.[40]

Blends to be used for melting experiments were obtained by the following procedure. Each methylene chloride solution of PDLA and PLLA was separately prepared to have a polymer concentration of 1 g/dL and then admixed with each other at 25 °C under vigorous stirring. The mixed solutions were cast onto a flat glass plate, and the solvent was allowed to evaporate at room temperature for ca. 1 week. The solvent molecules trapped in the resulting powders or films were extracted with methanol and dried in vacuo for another week. The obtained polymer powders or films were packed in a DSC aluminum cell and then sealed in test tubes under reduced pressure. The sealed samples were melted in an oil bath kept at 250 °C for 1 min and then immersed in an oil bath kept at given annealing temperatures (T_a) from 80 to 200 °C or quickly quenched to 0 °C.

Thermal Measurements and Optical Observations. The melting temperature (T_m) and the enthalpy of fusion (ΔH_m) were determined on the annealed blends with a Shimadzu DT-50 differential scanning calorimeter. They were heated under a nitrogen gas flow at a rate of 10 °C/min. We fixed the heating rate at 10 °C/min because higher rates such as 20 °C/min induced a T_m shift to higher temperature and lower rates such 5 °C/min resulted in thermal degradation of PLA because of long exposure to high temperature as mentioned below. T_m and ΔH_m were calibrated using indium as a standard. T_m and ΔH_m of indium are 156.4 °C and 3.26 kJ/mol, respectively.

The morphology of the annealed blends was studied with a Zeiss polarizing microscope. The samples for optical observation were prepared by the following procedure. A polymer powder or film was interposed between two micro cover glasses of 18 × 18 mm² and then sealed in a test tube under reduced pressure. The sealed samples were melted at 250 °C and then immersed for given periods of time in an oil bath thermostatically kept at a given T_a.

Results and Discussion

1. Thermal Degradation. Table II shows the percent weight loss of D1–L1, D5–L5, and D8–L8 when equimolar mixtures were heated at different T_a's for different annealing times (t_a). As is obvious, weight did not change at T_a below 140 °C, irrespective of t_a, while a significant weight loss was observed at T_a above 160 °C for t_a longer than 10 h. Remarkable weight loss at low molecular weights of PLA may be due to a high concentration of the terminal hydroxy group, as lactide monomers and cyclic oligomers seem to be formed from the terminal hydroxy group of the polymer chain.[41] Since thermal degradation is accelerated at high T_a but crystallization will proceed slowly at low T_a, 140 °C was selected as T_a for most of the annealing, unless otherwise specified.

Table II. Weight Loss (%) of D1–L1, D5–L5, and D8–L8 at Different T_a's for Different t_a's (X_D = 0.5)

T_a (°C)	D1–L1 t_a (h): 1	10	100	D5–L5 t_a (h): 1	10	100	D8–L8 t_a (h): 1	10	100
≤140	0	0	0	0	0	0	0	0	0
160	0	1	5	0	0	0	0	0	0
180	0	1	21	0	0	2	0	0	1
200	28	89	96	0	4	62	0	4	20

Table III. Characteristic Temperatures (°C) of Mixtures of D1 and L1 with Different X_D's for Different t_a's (T_a = 140 °C)

t_a (min)	X_D = 0: T_c	T_{m1}	X_D = 0.2: T_c	T_{m1}	T_{m2}	X_D = 0.5: T_c	T_{m2}	X_D = 0.8: T_c	T_{m1}	T_{m2}	X_D = 1: T_c	T_{m1}
0	81	157	74	127[a]	222	74	221	78	150	220	88	165
2	81	157	74	156	222		223	81	163	221	89	165
10	81	157	74	156	222		223		163	221	89	165
30	81	158	74	157	222				164	221	89	165
60	81	159	74	157	222		223		164	221		165
600		161		162	222		223		165	221		167

[a] A subpeak was observed at 155 °C.

DSC Study. There are at least four parameters which affect stereocomplexation of PDLA and PLLA from the melt: mixing ratio of the isomers (X_D), molecular weight of PDLA and PLLA ($\bar{M}_v$), annealing time (t_a), and annealing temperature (T_a).

1-1. Under Constant Molecular Weight. For simplicity, here only the polymer pair of D1 ($\bar{M}_v = 5.7 \times 10^3$) and L1 ($\bar{M}_v = 3.3 \times 10^3$) was employed.

(a) t_a Effect. Figure 1 shows the DSC thermograms of mixtures from D1 and L1 with various PDLA contents annealed at 140 °C for different t_a's. The PDLA content (X_D) was defined as follows:

$$X_D = \text{PDLA}/(\text{PDLA} + \text{PLLA}) \quad (2)$$

The results for X_D = 0 and 0.2 were similar to those for X_D = 1 and 0.8, respectively (data not shown). As seen from Figure 1a, the mixture with X_D = 0.5 and t_a = 0 shows an exothermic peak around 70 °C and an endothermic peak around 220 °C, while only one endothermic peak can be seen around 220 °C at t_a longer than 2 min. As reported elsewhere, the DSC peak at 220 °C is ascribed to melting of the racemic crystallites, while the peak at 170 °C is ascribed to melting of the homocrystallites of the homopolymer.[23] Therefore, all the mixtures with X_D = 0.5 must contain no homocrystallite, irrespective of t_a. The exothermic peak around 70 °C observed for the quenched sample (t_a = 0) disappears after annealing, though the melting peak of the racemic crystallites remains without any noticeable change. Thus, the exothermic peak around 70 °C can be assigned to crystallization of racemic crystallites during scanning. Such stereocomplexation during scanning was also reported for st- and it-PMMA by Schomacker and Challa.[42]

The crystallization temperature during scanning (T_c), the melting temperature of homocrystallites of PDLA or PLLA (T_{m1}), and the melting temperature of racemic crystallites (T_{m2}) evaluated from the DSC thermograms are given in Table III for different X_D's and different t_a's.

Table IV. Enthalpy Changes (J/g of Polymer) of Mixtures of D1 and L1 with Different X_D's for Different t_a's (T_a = 140 °C)

	X_D = 0		X_D = 0.2			X_D = 0.5		X_D = 0.8			X_D = 1	
t_a (min)	ΔH_c	H_{m1}	ΔH_c	ΔH_{m1}	ΔH_{m2}	ΔH_c	ΔH_{m2}	ΔH_c	ΔH_{m1}	ΔH_{m2}	ΔH_c	ΔH_{m1}
0	−55	54	−38	19	39	−52	80	−34	10	46	−57	57
2	−60	60	−26	28	39	0	87	−17	28	45	−55	55
10	−57	61	−24	33	39	0	84	0	26	43	−50	57
30	−37	60	−24	29	35			0	30	43	−26	65
60	−11	70	−18	29	34	0	90	0	29	43	0	73
600	0	77	0	37	38	0	90	0	31	42	0	80

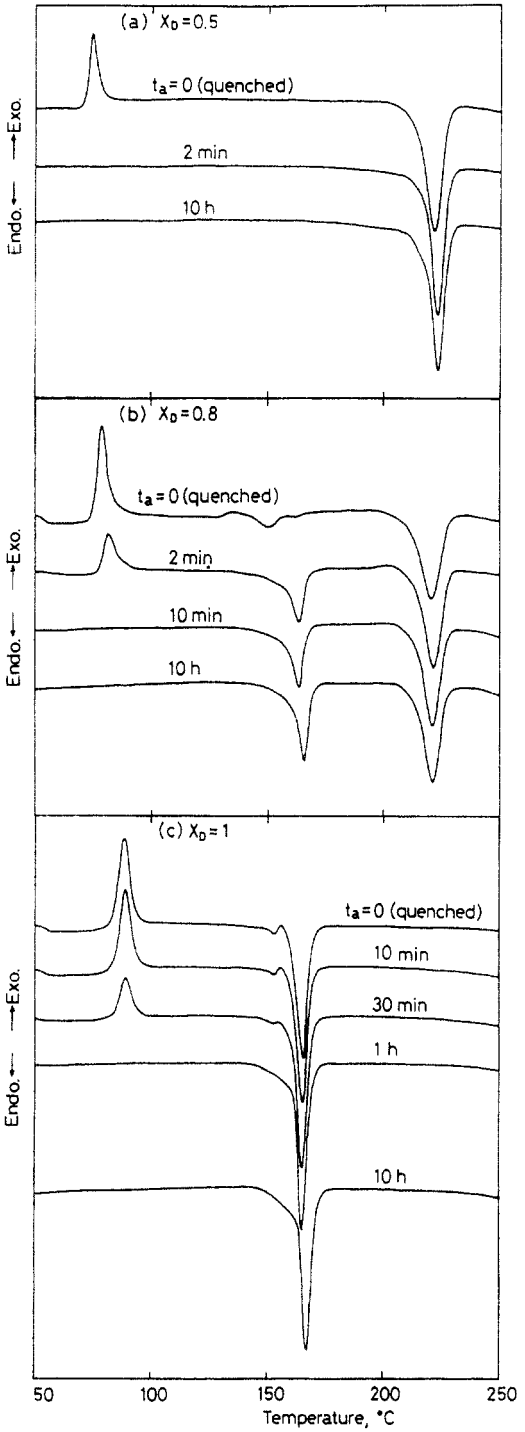

Figure 1. DSC thermograms of mixtures of D1 and L1 for different t_a's (T_a = 140 °C): (a): X_D = 0.5; (b) X_D = 0.8; (c) X_D = 1.

The enthalpy of crystallization during scanning (ΔH_c), the enthalpy of melting of homocrystallites (ΔH_{m1}), and the enthalpy of melting of racemic crystallites (ΔH_{m2}) are shown in Table IV. Theoretically, the sum of ΔH_{m1} and ΔH_{m2} should be equal to or larger than $|\Delta H_c|$, because crystallization takes place during annealing at T_a and scanning for the DSC measurement. The period of time during which the sum of ΔH_c, ΔH_{m1}, and ΔH_{m2} practically remains zero is defined here as the induction period of crystallization (t_i). According to this definition, t_i for X_D = 0.5 is 0. This means that the induction period of racemic crystallization is shorter than the quenching time (a few seconds). In other words, the racemic crystallization including nucleation and growth proceeds in a few seconds. Therefore, the melting peak observed around 220 °C for t_a = 0 is due to the racemic crystallites formed during quenching and scanning. As the crystallization peak around 70 °C disappears upon annealing for 2 min, the melting peak around 220 °C for t_a longer than 2 min is due to the racemic crystallites formed during annealing. An insignificant increase of T_{m2} and ΔH_{m2} for X_D = 0.5 after 2 min suggests that racemic crystallization comes to an end in a short annealing time. The largest ΔH_{m2} observed for the stereocomplex from the melt (90 J/g of polymer) is smaller than that previously found for the stereocomplex formed in acetonitrile solution (100 J/g of polymer).[27] This may be explained in terms of crystallinity which must be higher for the complex formed in the presence of solvent than that from the melt. Solvent may help the polymer segments to diffuse to the growth site of the racemic crystallites, resulting in formation of a highly ordered stereocomplex.

On the other hand, as seen from Figure 1c, nonblended PLA (D1 alone) has an exothermic peak around 90 °C and an endothermic peak around 170 °C when t_a is shorter than 30 min. The former and the latter peaks are ascribed to crystallization and melting of hoocrystallites of PDLA, respectively. As seen from Table IV, the sum of ΔH_c and ΔH_{m1} for L1 (X_D = 0) and D1 (X_D = 1) becomes positive at t_a = 10 min. Tables III and IV show an increase in both T_{m1} and the sum of ΔH_c and ΔH_{m1} for t_a from t_i to 10 h. These results support the above assumption that homocrystallization requires a longer induction time than for the racemic crystallization.

When D1 and L1 were mixed at a nonequimolar ratio (X_D = 0.8, Figure 1b), peaks were observed around 80 (crystallization), 160 (melting of homocrystallites), and 220 °C (melting of racemic crystallites). As the sum of ΔH_c, ΔH_{m1}, and ΔH_{m2} gives a positive value for t_a = 0, the quenched sample must already contain crystallites with t_i shorter than the quenching time. Both the crystallites formed during quenching and scanning have their melting peaks for t_a = 0 and 2 min. As ΔH_{m1} is much smaller than ΔH_{m2} for t_a = 0, the amount of racemic crystallites formed during quenching and scanning is much larger than that of homocrystallites. An imperfect melting peak observed at 170 °C for t_a = 0 suggests that the quenching and scanning times are not sufficiently long to complete homocrystallization. Disappearance of the crystallization peak for t_a longer than 10 min indicates occurrence of crystallization during annealing. Independence of T_{m2} and ΔH_{m2} on t_a together with the disappearance of the crystallization peak for t_a longer than 10 min for X_D = 0.8 suggests that racemic crystallization is completed in 10

Table V. T_{m1} (°C), T_{m2} (°C), ΔH_{m1} (J/g of Polymer), and ΔH_{m2} (J/g of Polymer) of L1 (X_D = 0), an Equimolar Mixture of D1 and L1 (X_D = 0.5), and D1 (X_D = 1) for Different T_a's (t_a = 10 h)

	X_D = 0		X_D = 0.5		X_D = 1	
T_a (°C)	T_{m1}	ΔH_{m1}	T_{m2}	ΔH_{m2}	T_{m1}	ΔH_{m1}
80	158	62	223	80	165	60
100	158	73	223	85	164	74
120	157	75	223	83	164	75
140	161	77	223	90	167	80
160			220[a]	88[a]		
180			219[a]	89[a]		
200			b	b		

[a] Weight loss occurred during annealing. [b] Unmeasurable because most of the sample weight was lost due to thermal degradation.

min of annealing. An increase in T_{m1} and ΔH_{m1} for t_a from 10 min to 10 h for X_D = 0.8 indicates that homocrystallization proceeds for longer than 10 h. Racemic crystallization again is completed in a much shorter time than homocrystallization at X_D = 0.8. This trend was also observed at X_D = 0.2, which has the same enantiomeric excess value as X_D = 0.8. The excess component which forms homocrystallites following completion of racemic crystallization is D1 for X_D = 0.8 and L1 for X_D = 0.2. It is evident from the T_{m1} data at 10 h (Table III) that T_{m1} at X_D = 0.2 and 0.8 is very similar to that at X_D = 0 and 1, respectively. T_{m1} of D1 (X_D = 1) is higher than that of L1 (X_D = 0), and undercooling at 140 °C for D1 (excess crystallizable component at X_D = 0.8) is higher than that for L1 (excess crystallizable component at X_D = 0.2) probably because of a slightly higher $\bar{M}_v$ and $[\alpha]^{25}_D$ of D1 than L1. This may be also the reason for faster completion of the crystallization at X_D = 0.8 than at X_D = 0.2.

(b) T_a Effect. Table V shows T_m and ΔH_m for the mixtures with X_D = 0, 0.5, and 1 annealed at different T_a's for t_a = 10 h. No crystallite was formed above 160 °C when X_D was 0 and 1. For the equimolar mixture an amount of polymer necessary for DSC measurement could not be obtained at high annealing temperatures like 200 °C, because a significant weight loss took place by thermal degradation. Racemic crystallization at X_D = 0.5 seems to be insignificantly affected by T_a, as T_{m2} remains constant, though a slight decrease in ΔH_{m2} with decreasing T_a is seen. In contrast, T_{m1} of the polymers at X_D = 0 and 1 is higher when T_a = 140 °C than when T_a < 120 °C, and ΔH_{m1} decreases with a decrease in T_a, suggesting the crystalline size and crystallinity of the single polymer decrease with decreasing T_a.

(c) X_D Effect. T_{m1} and T_{m2} of the mixtures of D1 and L1 annealed at 140 °C for 10 h are plotted as a function of X_D in Figure 2a. As seen, the mixtures with X_D between 0.1 and 0.3 and between 0.7 and 0.9 have both T_{m1} and T_{m2}, but the mixtures with X_D ranging between 0.4 and 0.6 have only T_{m2}. T_{m2} becomes maximum at X_D around 0.5, whereas T_{m1} remains constant around 160 °C for X_D between 0 and 0.3 and around 165 °C for X_D between 0.7 and 1, though a slight rise is observed with an increase in X_D. The higher T_{m1} for X_D between 0.7 and 1 than that between 0 and 0.3 is probably due to the higher optical purity and the higher molecular weight of D1 than those of L1.

ΔH_{m1} and ΔH_{m2} for the mixtures of D1 and L1 annealed at 140 °C for 10 h are plotted as a function of X_D in Figure 2b. As is obvious, the maximum ΔH_{m2} is observed exactly at X_D = 0.5, similar to crystallization in the casting[25] and the nonsolvent precipitating method.[26] It is interesting to note that solely racemic crystallites are formed at X_D = 0.4 and 0.6 although they are not equimolarly mixed. The excess component may be trapped in the boundary of the formed racemic crystallites without sufficient space for homocrystallization.

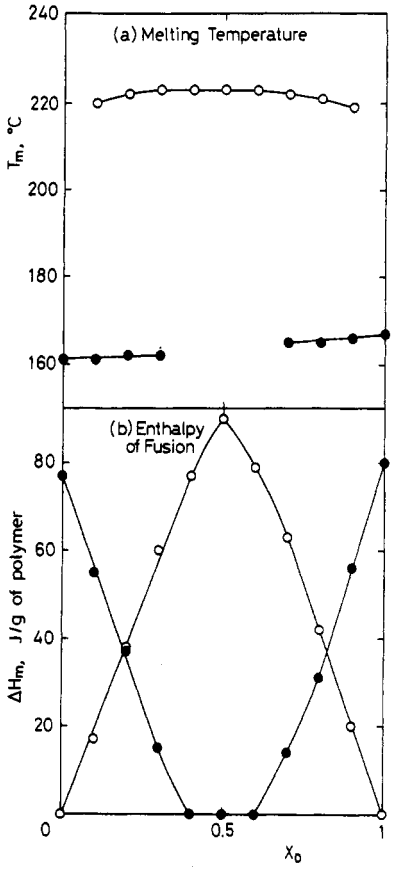

Figure 2. T_{m1} (●), T_{m2} (○), ΔH_{m1} (●), and ΔH_{m2} (○) evaluated from DSC thermograms of mixtures of D1 and L1 as a function of X_D (T_a = 140 °C, t_a = 10 h).

When mixtures of different X_D were annealed at 80 °C, the dependence of T_m and ΔH_m on X_D showed a tendency similar to that at T_a = 140 °C (data not shown), though T_{m1}, ΔH_{m1}, and ΔH_{m2} were lower than those at 140 °C. In the case of PMEPL, the effect of enantiomeric excess-(=|*R*-polymer − *S*-polymer|/(*R*-polymer + *S*-polymer) or |D-polymer − L-polymer|/(D-polymer + L-polymer)) on the melting temperature and the enthalpy of fusion of the stereocomplex and the homocrystallites of either (*S*)-(−)-PMEPL or (*R*)-(+)-PMEPL was similar to that for the mixtures of PDLA and PLLA.[19] The only difference was that the critical enantiomeric excess, above which homocrystallites were also formed, was lower for PLA blends (ca. 0.4) than that for PMEPL blends (ca. 0.5). The stereocomplexation of PMEPL is likely to more strongly hinder homocrystallization than that of PLA.[19]

1-2. Under Constant Mixing Ratio (X_D = 0.5). (a) t_a Effect. Figure 3 shows the DSC thermograms for equimolar mixtures of D1–L1, D5–L5, and D8–L8 obtained at T_a = 140 °C for different t_a. T_c, T_{m1}, and T_{m2} and ΔH_c, ΔH_{m1}, and ΔH_{m2} estimated from the DSC thermograms are given in Tables VI and VII, respectively. As mentioned above, racemic crystallites are formed for D1–L1 during a short quenching time such as a few seconds and during scanning of the DSC measurement. Crystallization was completed within 2 min of annealing.

Quenching of D5–L5 yields a crystallization peak around 110 °C and melting peaks of homocrystallites and racemic crystallites around 180 and 230 °C, respectively (Figure 3b). The sum of ΔH_c, ΔH_{m1}, and ΔH_{m2} for t_a = 0 amounts to +6 J/g of polymer (Table VII), showing that the

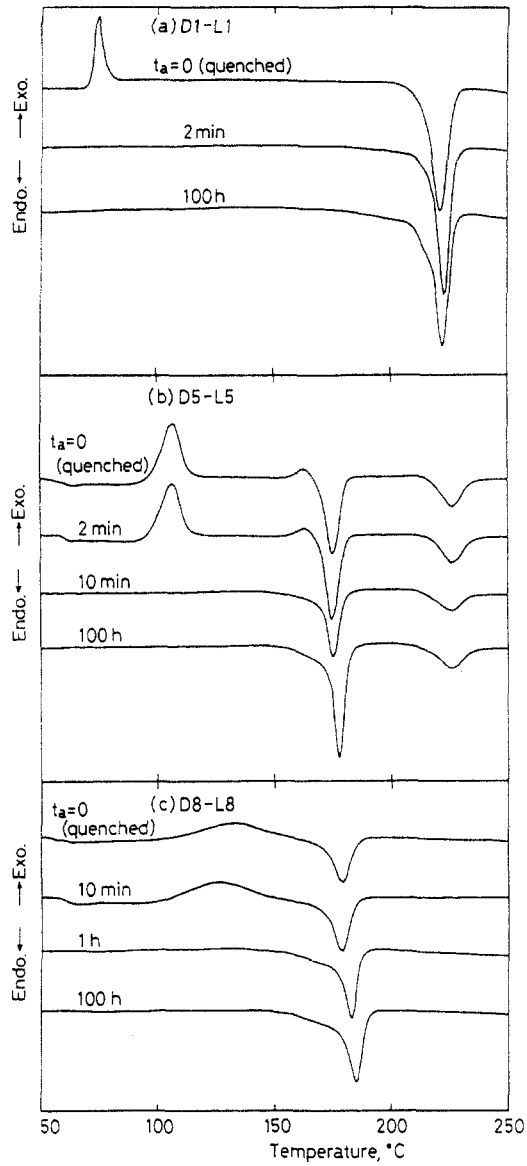

Figure 3. DSC thermograms of equimolar mixtures of PDLA and PLLA for different t_a's (T_a = 140 °C): (a): D1–L1; (b) D5–L5; (c) D8–L8.

Table VI. Characteristic Temperatures (°C) of D1–L1, D5–L5, and D8–L8 for Different t_a's (X_D = 0.5, T_a = 140 °C)

	D1–L1		D5–L5			D8–L8	
t_a (min)	T_c	T_{m2}	T_c	T_{m1}	T_{m2}	T_c	T_{m1}
0	74	221	107	175	226	132	179
2		223	106	174	226		
10		223		174	226	127	178
60		223		176	226		183
600		223		176	226		184
6000		220		177	226		185

Table VII. Enthalpy Changes (J/g of Polymer) of D1–L1, D5–L5, and D8–L8 for Different t_a's (X_D = 0.5, T_a = 140 °C)

	D1–L1		D5–L5			D8–L8	
t_a (min)	ΔH_c	ΔH_{m2}	ΔH_c	ΔH_{m1}	ΔH_{m2}	ΔH_c	ΔH_{m1}
0	−52	80	−51	36	23	−31	32
2	0	87	−46	38	22	−34	34
10	0	84	0	50	23	−36	37
60	0	90	0	58	24	0	52
600	0	90	0	60	24	0	55
6000	0	87	0	64	22	0	57

quenched mixture already contains a small amount of crystallites. The homocrystallites and racemic crystallites for t_a = 0 must be mainly formed during quenching and DSC scanning. The crystallization peak around 110 °C disappears by annealing for 10 min, but homocrystallization requires a longer time, because T_{m1} and ΔH_{m1} continue to increase with annealing. In contrast, racemic crystallization comes to completion by annealing for 2 min as T_{m2} and ΔH_{m2} remain constant, irrespective of annealing time. Homocrystallites formed in D5–L5 must be composed of two kinds of homocrystallites from D- and L-polymer, *in contrast with those formed at nonequimolar* mixing ratios where homocrystallites are composed of excess D- or L-polymer.

Table VIII. Enthalpy Changes (J/g of Polymer) of D1–L1, D5–L5, and D8–L8 at Different T_a's (X_D = 0.5, t_a = 10 h for D1–L1, t_a = 100 h for D5–L5 and D8–L8)

T_a	D1–L1			D5–L5			D8–L8		
(°C)	ΔH_c	ΔH_{m1}	ΔH_{m2}	ΔH_c	ΔH_{m1}	ΔH_{m2}	ΔH_c	ΔH_{m1}	ΔH_{m2}
80	0	0	80						
100	0	0	85	0	44	23	0	33	0
120	0	0	83	0	50	22	0	47	0
140	0	0	90	0	64	22	0	57	0
160	0[a]	0[a]	88[a]	0	60	20	0	66	0
180	0[a]	0[a]	89[a]	15[a]	29[a]	40[a]	6[a]	53[a]	9[a]
200	*b*	*b*	*b*	0[a]	0[a]	38[a]	0[a]	0[a]	80[a]

[a] Weight loss occurred due to thermal degradation. [b] Unmeasurable because most of the sample weight was lost due to thermal degradation.

The D8–L8 mixture gives more diffuse crystallization and melting peaks upon quenching than D1–L1 and D5–L5 (Figure 3c). The sum of ΔH_c and ΔH_{m1} amounts to approximately zero, strongly suggesting that the quenched mixture is amorphous. The endothermic peak around 180 °C for t_a = 0 must be due to melting of the homocrystallites formed around 130 °C during DSC scanning. The diffuse crystallization peak disappears when D8–L8 is annealed for 1 h, but T_{m1} and ΔH_{m1} slightly increase with annealing. Also in this case homocrystallites must be composed of two kinds of homocrystallites from D- and L-polymer.

The above findings indicate that racemic crystallization is replaced by homocrystallization when the molecular weight of PDLA and PLLA becomes higher.

(b) T_a Effect. ΔH_c, ΔH_{m1}, and ΔH_{m2} evaluated from the DSC thermograms of D1–L1, D5–L5, and D8–L8 annealed at different T_a's are given in Table VIII. t_a was 10 h for D1–L1 and 100 h for D5–L5 and D8–L8. In the case of D1–L1, only ΔH_{m2} is observed over T_a from 80 to 180 °C, indicating exclusive formation of racemic crystallites. On the other hand, homocrystallization also occurs in D5–L5. As D5–L5 undergoes thermal degradation at T_a above 180 °C, the decrease in molecular weight caused by thermal degradation at high T_a might have accelerated racemic crystallization, resulting in a ΔH_{m2} increase and a ΔH_{m1} decrease at T_a above 180 °C. The D8–L8 mixture shows a similar dependence of ΔH_{m1} and ΔH_{m2} on T_a above 180 °C. Formation of racemic crystallites only at high T_a may be due to the decrease in molecular weight at high T_a. Since the reduction of polymer molecular weight due to random degradation must be larger for higher molecular weight PLA, crystallization of D8–L8 may be more greatly affected by high-temperature annealing than that of D5–L5.

T_{m1} and T_{m2} estimated from the DSC thermograms of D1–L1, D5–L5, and D8–L8 annealed at different T_a's are plotted in Figure 4 as a function of T_a. t_a was 10 h for D1–L1 and 100 h for D5–L5 and D8–L8. As is seen, T_{m2} of D1–L1 remains constant, independent of T_a. Extrapolation of the straight line to $T_m = T_a$ gives the equilibrium melting temperature of the racemic crystallites (T^0_{m2}). In the case of D5–L5, T_{m2} is constant below 140 °C, but

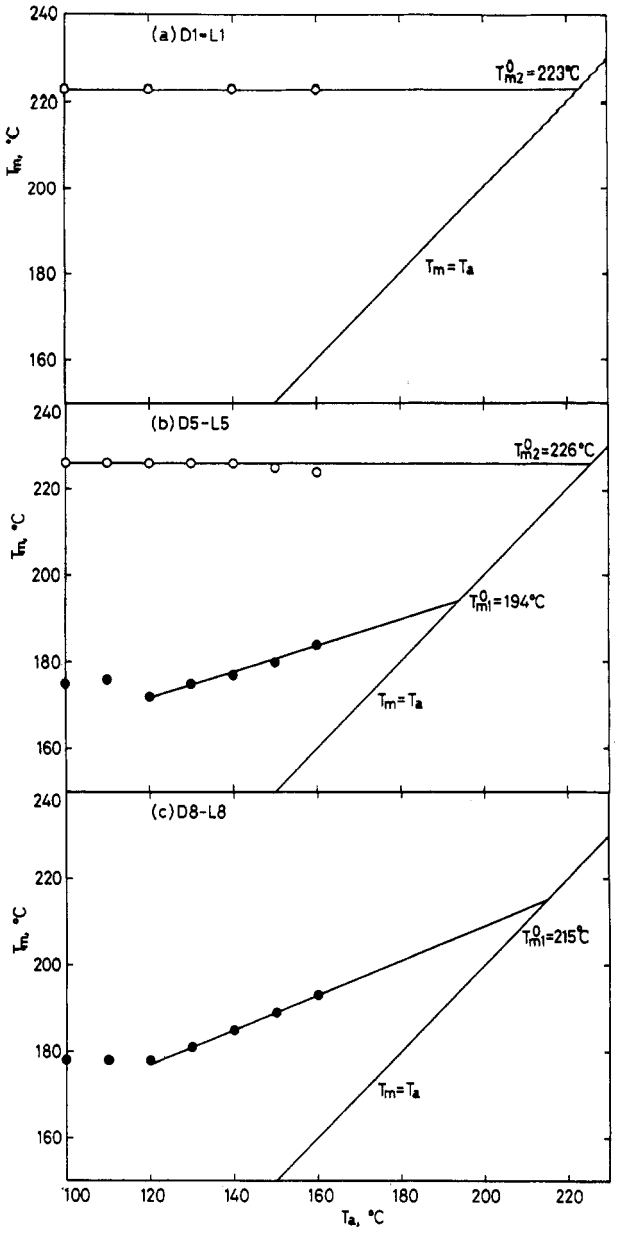

Figure 4. T_{m1} (●) and T_{m2} (○) evaluated from DSC thermograms of equimolar mixtures of PDLA and PLLA as a function of T_a: (a) D1–L1 (t_a = 10 h); (b) D5–L5 (t_a = 100 h); (c) D8–L8 (t_a = 100 h).

slightly decreases with increasing T_a above 140 °C, probably because of thermal degradation at high T_a. Extrapolation of T_{m2} to $T_m = T_a$ for T_a below 140 °C yields 226 °C as T^0_{m2}, which is slightly higher than T^0_{m2} of D1–L1. The shorter molecular chain may lower the size of the racemic crystallites and increase the crystalline structure defects due to a higher concentration of the terminal group. In contrast, T_{m1} of D5–L5 increases linearly with an increase in T_a, and extrapolation of the experimental data to $T_m = T_a$ gives 194 °C as the equilibrium melting point of the homocrystallites (T^0_{m1}). In this procedure the data for T_a lower than 120 °C were neglected because it was apparent from DSC curves that recrystallization of the homocrystallites occurred during scanning, resulting in a higher T_{m1} than the true value (data not shown). The estimated T^0_{m1} is lower than 215 °C, which is reported for PLLA by Kalb and Pennings.[43] Homocrystallization may be hindered by the concomitant racemic crystallites, or D5 and L5 with a molecular weight much lower than the 5.5×10^5 of PLLA employed by Kalb and Pennings might

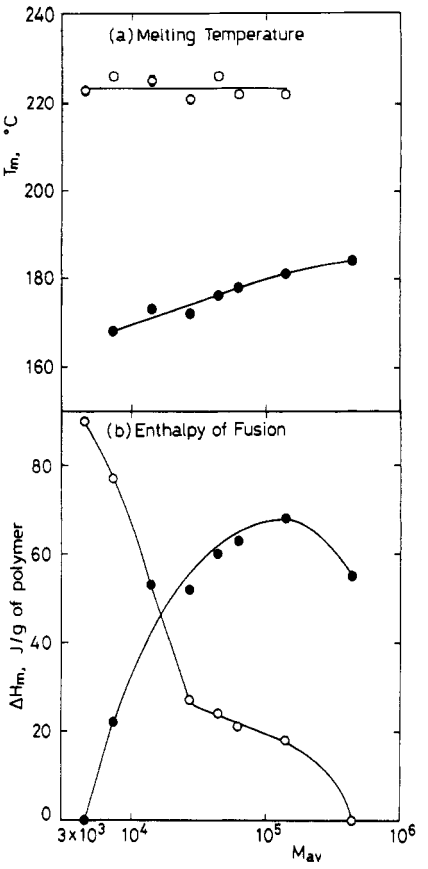

Figure 5. T_{m1} (●), T_{m2} (○), ΔH_{m1} (●), and ΔH_{m2} (○) evaluated from DSC thermograms of equimolar mixtures of PDLA and PLLA as a function of M_{av} (T_a = 140 °C, t_a = 10 h).

reduce the size of the homocrystallites, resulting in a lower T^0_{m1}.

T_{m1} of D8–L8 also gives a linear relation with T_a, at least above 130 °C as seen from Figure 4c. Extrapolation of the straight line to $T_m = T_a$ yields 215 °C as T^0_{m1}, which is in good agreement with the reported value for single PLLA (215 °C).[43] This suggests that homocrystallization of the mixtures of PDLA and PLLA from the melt proceeds without any particular interaction between PDLA and PLLA, similar to the nonblended PLA melt, so long as both PDLA and PLLA have a molecular weight higher than 4×10^5. The data for T_a lower than 120 °C were also neglected for the same reason as that for D5–L5.

(c) M_{av} Effect. Figure 5a shows T_{m1} and T_{m2} evaluated from the DSC thermograms of D1–L1, D2–L2, D3–L3, D4–L4, D5–L5, D6–L6, D7–L7, and D8–L8 annealed at 140 °C for 10 h as a function of the arithmetically averaged molecular weight of PDLA and PLLA (M_{av}). The approximately constant T_{m2} implies that the size of the racemic crystallites formed from the melt is independent of the molecular weight of PLA. In contrast, T_{m1} becomes higher with increasing M_{av}, probably because the size of the homocrystallites becomes larger with increasing M_{av}. ΔH_{m1} and ΔH_{m2} of D1–L1, D2–L2, D3–L3, D4–L4, D5–L5, D6–L6, D7–L7, and D8–L8 annealed at 140 °C for 10 h are given in Figure 5b as a function of M_{av}. Apparently, ΔH_{m1} increases whereas ΔH_{m2} decreases with an increase in M_{av}, indicating that racemic crystallites and homocrystallites are predominantly formed at lower and higher molecular weight, respectively. The effect of PLA molecular weight on the crystallization from the melt is very similar to that from casting (solvent evaporation), though the critical molecular weight (M_c), below which only the racemic crystallites are formed, is lower for the crystal-

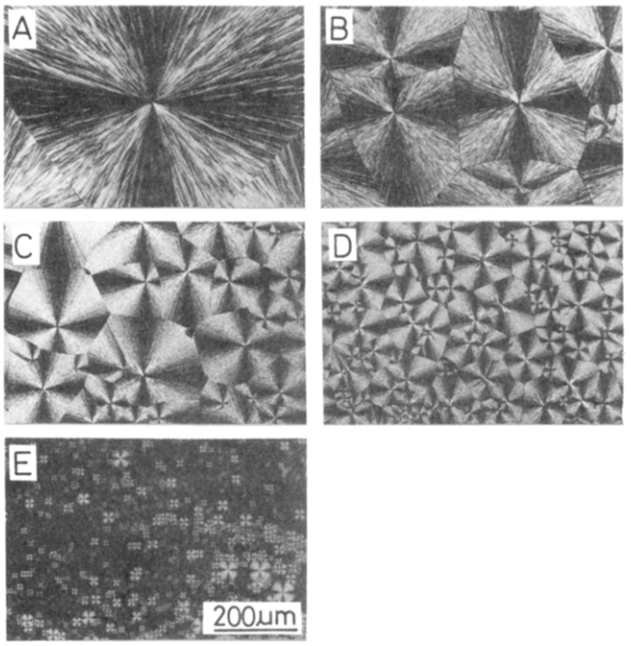

Figure 6. Photomicrographs of the equimolar mixture of D1 and L1 at different T_a's for different t_a's (X_D = 0.5): (A) T_a = 180 °C for 1 h; (B) T_a = 160 °C for 1 h; (C) T_a = 140 °C for 10 h; (D) T_a = 80 °C for 10 h; (E) quenched.

lization from the melt (6×10^3) than 4×10^4 observed for that from the solution casting.[25]

2. Morphology of Spherulites. 2-1. Under Constant Molecular Weight. (a) T_a Effect. Figure 6 shows photomicrographs of the spherulites formed from D1–L1 with X_D = 0.5 annealed at different T_a's, together with the quenched sample. t_a was 10 h for T_a between 80 and 140 °C and 1 h for T_a of 160 and 180 °C to avoid thermal degradation at high temperatures. These spherulites are composed entirely of racemic crystallites, because the above DSC measurements revealed that these annealed mixtures contain only racemic crystallites. Obviously, even the quenched mixture produces spherulites to suggest that nucleation for racemic crystallization proceeds very quickly. This is in good agreement with the above DSC results. The average radius of the formed racemic crystalline spherulites markedly decreases with a decrease in T_a. The spherulites formed at 180, 160, 140, and 80 °C have an average radius of 300, 200, 100, and 50 μm, respectively. The lower density of the crystal nucleus at higher T_a will increase the average radius of the racemic crystalline spherulites. As seen from Table V and Figure 6, the melting temperature of racemic crystallites (T_{m2}) is independent of the size of the spherulites.

To compare the morphology of the spherulites of the homocrystallites, they were prepared from nonblended samples of L1 (X_D = 0) and D1 (X_D = 1) under the same annealing conditions of equimolar D1–L1. The photomicrographs of L1 and D1 obtained at T_a = 140 °C and those of D1 annealed at T_a from 140 to 80 °C are given in Figures 7 and 8. In contrast with the mixture of X_D = 0.5, no homocrystallite was formed at T_a above 160 °C as expected. T_a = 160 °C is very close to T_{m1} of L1 (161 °C) and D1 (167 °C). However, large spherulites with an average radius of ca. 2 mm were formed from L1 and D1 at T_a = 140 °C. The slight difference in size and morphology observed between L1 and D1 may be due to the difference in $\bar{M}_v$ and optical purity of the polymers. As seen in Figure 8, the average radius of spherulites of D1 dramatically decreases from 2 mm (T_a = 140 °C) to 10 μm (T_a = 80 °C). At T_a = 140 °C, the homocrystalline

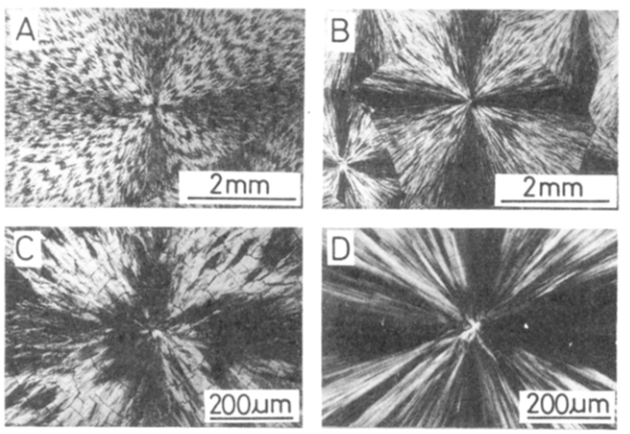

Figure 7. Photomicrographs of single polymers of D1 and L1 (T_a = 140 °C, t_a = 10 h): (A) L1; (B) D1; (C) magnification of (A); (D) magnification of (B).

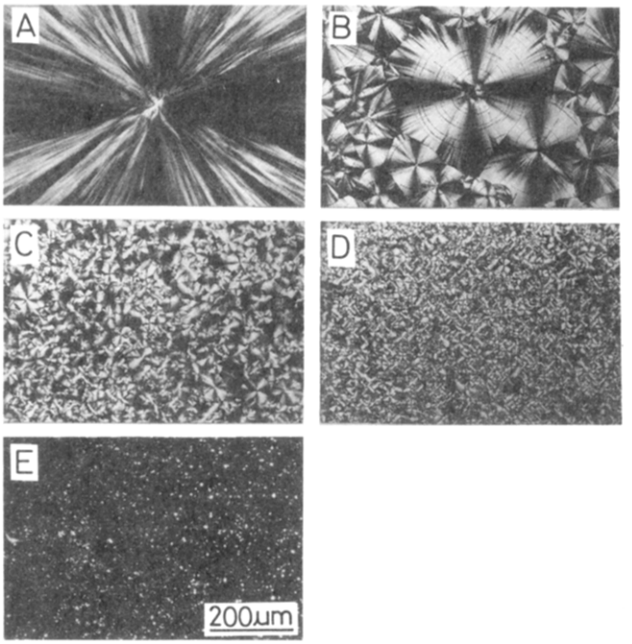

Figure 8. Photomicrographs of D1 single polymers annealed at various T_a's (t_a = 10 h): (A) T_a = 140 °C; (B) T_a = 120 °C; (C) T_a = 100 °C; (D) T_a = 80 °C; (E) quenched.

spherulites have an average radius (2000 μm) that is an order of magnitude larger than that of the racemic crystalline spherulites (200 μm). This ratio is reversed at T_a = 100 °C, probably because the dependence of nucleus density of homocrystallites on T_a is much stronger than that of racemic crystallites. As seen from Table V and Figure 8, the melting temperature of the homocrystallites of L1 and D1 is independent of the size of the spherulites at T_a below 120 °C.

The photograph of the quenched polymer (Figure 8E) was taken focusing on an area containing an enormously large number of microhomocrystallites compared with the normal area in the sample, as no photographs could be taken in the normal area because of very low light density due to the very low amount of the homocrystallites. This is in agreement with the DSC result.

As for the spherulites of PLLA, Fischer et al. reported that annealing of L-rich D,L-lactide copolymer ($\bar{M}_v$ = (0.8–1.0) × 10^5) containing 3.65% D-unit at 130 °C from the melt resulted in the formation of spherulites having an average radius of 50 μm.[44] Kalb and Pennings also showed the formation of spherulites with a radius of 50 μm by annealing of PLLA ($\bar{M}_v$ = 5.5 × 10^5) at 120 °C from the

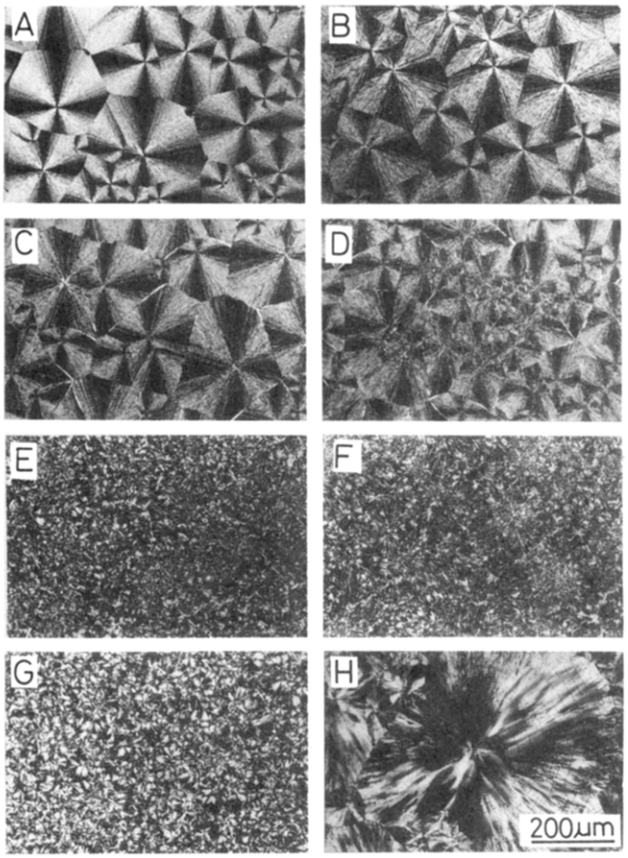

Figure 9. Photomicrographs of mixtures of D1 and L1 with different X_D's (T_a = 140 °C, t_a = 10 h): (A) X_D = 0.5; (B) X_D = 0.6; (C, D) X_D = 0.7; (E) X_D = 0.8; (F–H) X_D = 0.9.

melt.[43] These radii are of the same order as those of our PDLA spherulites formed by annealing at 120 °C. Further, Vasanthakumari and Pennings revealed that well-defined spherulites, coarsely grained spherulites, axialities, and single crystals were formed from PLLA ($\bar{M}_v$ = (0.68–6.9) × 10^5) melt by varying the annealing temperature and polymer molecular weight.[45] The polymer molecular weight and melting conditions employed in these investigations are different from ours.

The radius of these PLA racemic crystalline spherulites is of the same order as that of (*S*)-(−)-PMEPL and (*R*)-(+)-PMEPL reported by Grenier and Prud'homme (500 μm).[19] In their study, spherulites were formed at a constant rate of temperature decrease from the melt. The size of the homocrystalline spherulites of (*S*)-(−)-PMEPL or (*R*)-(+)-PMEPL was much smaller than that of the racemic crystalline spherulites.[19] When our PLA spherulites were allowed to form under a constant rate of temperture decrease, the difference in radius between the racemic crystalline and the homocrystalline spherulites was very similar to that of PMEPL. Annealing under a constant rate of temperature decrease gave racemic crystalline spherulites with an average radius of ca. 100 μm, which was larger than that of the homocrystalline spherulites of PDLA or PLLA (about 10 μm) (photographs not shown).

(b) X_D Effect. Figure 9 shows photomicrographs of the mixtures of D1 and L1 with various X_D's annealed at 140 °C for 10 h. As seen from Figure 9A,B the spherulites formed at X_D = 0.6 have a size dispersion similar to those at X_D = 0.5. These spherulites are also composed of racemic crystallites alone, because the DSC measurement revealed that the blend of X_D = 0.6 contains only racemic crystallites. The lower contrast between the light and dark regions in the spherulites of X_D = 0.6 than those of

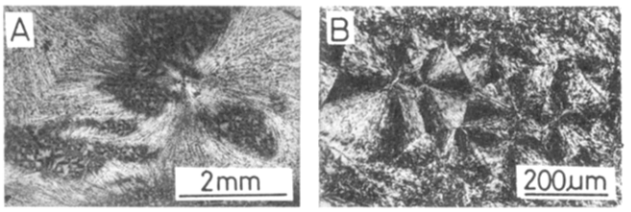

Figure 10. Photomicrographs of the mixtures of D1 and L1 with X_D of 0.1 (T_a = 140 °C, t_a = 10 h). (B) is a magnification of (A).

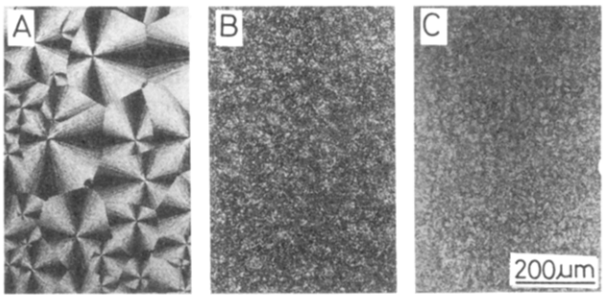

Figure 11. Photomicrographs of equimolar mixture of PDLA and PLLA with different M_a's (X_D = 0.5, T_a = 140 °C, T_a = 10 h): (A) D1–L1 (M_{av} = 4.5 × 10^3); (B) D5–L5 (M_{av} = 4.4 × 10^4); (C) D8–L8 (M_{av} = 4.4 × 10^5).

X_D = 0.5 suggests that the spherulites formed under the nonequimolar condition are more defective in crystalline structure or more irregular in orientation of the lamellas than those formed under the equimolar condition. The defect or irregularity of spherulites may also be the reason for a lower ΔH_{m2} at X_D = 0.6 than at X_D = 0.5. At X_D = 0.7, relatively well-ordered spherulites are observed together with rather disordered or defective spherulites. The latter may contain homocrystallites. Lower T_{m2} and ΔH_{m2} at X_D = 0.7 than at X_D = 0.5 and 0.6 must also be due to irregularity of the crystalline structure or smaller size of the respective crystallites composing the spherulites. At X_D = 0.8, most parts (about 100 μm) become dark with very small bright parts (about 10 μm), and spherulites cannot be observed. However, large homocrystalline spherulites appear when X_D becomes 0.9. The bright parts observed for the mixtures of X_D = 0.8 and 0.9 are much like the homocrystallites of D1 at T_a = 80 °C. Thus the bright part is likely to be composed mostly of homocrystallites, whereas the dark part consists of racemic crystallites.

The results obtained for X_D = 0.6, 0.7, 0.8, and 0.9 were very similar to those for X_D = 0.4, 0.3, 0.2, and 0.1, respectively, though the mixtures of X_D = 0.1 and 0.2 contained regions composed of racemic crystalline spherulites in addition to the regions observed for X_D = 0.9 (Figure 9F–H) and 0.8 (Figure 9E), respectively. The region which was formed at X_D = 0.1 and contained racemic crystalline spherulites is given in Figure 10. As seen from Figure 10B, the racemic crystalline spherulites (relative dark parts) are much disordered and dispersed in the homocrystalline spherulites (relative light parts). As the molecular weight of L1 is lower than that of D1, higher molecular mobility in blends at X_D = 0.1 and 0.2 than at X_D = 0.9 and 0.8 may enhance the diffusion of molecules toward the growth sites of racemic crystalline spherulites, resulting in formation of clear racemic crystalline spherulites.

2-2. Under Constant Mixing Ratio (X_D = 0.5). Photomicrographs of equimolar D1–L1, D5–L5, and D8–L8 annealed at 140 °C for 10 h are shown in Figure 11. Spherulites with an average radius ranging from 20 to 100

μm are clearly observed for D1–L1, whereas merely a large number of small-sized crystallites are seen for D5–L5 and D8–L8. As described above, D1–L1 yields exclusively racemic crystallites and D8–L8 only homocrystallites, while D5–L5 produces both racemic crystallites and homocrystallites. The morphology of D5–L5 (Figure 11B), composed of relatively light and dark regions, is very similar to that of nonequimolar mixtures of D1 and L1 such as X_D = 0.8 shown in Figure 9E, though their crystal sizes are different from one another. As mentioned above, the light and dark parts in Figure 9E may be mostly composed of homocrystallites and racemic crystallites, respectively. This composition may also be valid for D5–L5. Though D8–L8 contains solely homocrystallites, they are not clearly observed, probably due to the high molecular weight of D8 and L8.

Concluding Remarks

The above DSC study revealed that annealing of melt blends from PDLA and PLLA resulted in formation of large amounts of racemic crystallites as the mixing ratio approached 1:1 and the molecular weight of both polymers was as low as 10^3. When the mixing ratio of the melt deviated from equimolar blending or the molecular weight of the polymer was higher than 10^4, both racemic crystallites and homocrystallites were simultaneously formed. Polarizing microscopic observation of the annealed mixtures clearly exhibited that they were composed of spherulites. In some cases, crystallization took place during scanning for the DSC measurements. The melting temperature of the racemic crystallites was independent of the size of the spherulites but decreased as the melt blend deviated from the equimolar mixing. This may be ascribed to a disordered crystalline structure or a smaller size of the respective crystallites composing the spherulites but not the size of the spherulites themselves. The disordered region of the spherulites was likely to contain small homocrystallites.

Acknowledgment. We wish to thank the Laboratory of Plant Chemistry in the Institute for Chemical Research, Kyoto University, for the use of the polarimeter facility. We are also grateful to Mr. Teruhiko Kawanishi (Research Center for Chemometrics, Toyohashi University of Technology) and Mr. Hirokazu Muramoto (Technology Development Center, Toyohashi University of Technology) for their help with the polarizing microscopic observation.

References and Notes

(1) Tsuboi, M.; Wada, A.; Nagashima, N. *J. Mol. Biol.* **1961**, *3*, 705.
(2) Tsuboi, M.; Mitsui, Y.; Wada, A.; Miyazawa, T.; Nagashima, N. *Biopolymers* **1963**, *1*, 297.
(3) Tsuboi, M. *Biopolymers* **1964**, *Symposia No. 1*, 527.
(4) Elliott, A.; Fraser, R. D. B.; MacRae, T. P. *J. Mol. Biol.* **1965**, *11*, 821.
(5) Mitsui, Y.; Iitaka, Y.; Tsuboi, M. *J. Mol. Biol.* **1967**, *24*, 15.
(6) Squire, J. M.; Elliott, A. *Mol. Cryst. Liq. Cryst.* **1969**, *7*, 457.
(7) Squire, J. M.; Elliott, A. *J. Mol. Biol.* **1972**, *65*, 291.
(8) Tsuchiya, S.; Watanabe, J.; Uematsu, Y.; Uematsu, I. *Rep. Prog. Polym. Phys. Jpn.* **1972**, *15*, 637.
(9) Masuko, S.; Tsujita, Y.; Uematsu, I. *Rep. Prog. Polym. Phys. Jpn.* **1973**, *16*, 611.
(10) Takahashi, T.; Tsutsumi, A.; Hikichi, K.; Kaneko, M. *Macromolecules* **1974**, *7*, 806.
(11) Fukuzawa, T.; Uematsu, I.; Uematsu, Y. *Polym. J.* **1974**, *6*, 537.
(12) Yoshikawa, M.; Tsujita, Y.; Uematsu, I.; Uematsu, Y. *Polym. J.* **1975**, *7*, 96.
(13) Matsushima, N.; Hikichi, K.; Tsutsumi, A.; Kaneko, M. *Polym. J.* **1975**, *7*, 382.
(14) Baba, Y.; Kagemoto, A. *Macromolecules* **1977**, *10*, 458.
(15) Yoshida, T.; Sakurai, S.; Okuda, T.; Takagi, Y. *J. Am. Chem. Soc.* **1962**, *84*, 3590.
(16) Dumas, P.; Spassky, N.; Sigwalt, P. *Makromol. Chem.* **1972**, *156*, 55.
(17) Sakakihara, H.; Takahashi, Y.; Tadokoro, H.; Oguni, N.; Tani, H. *Macromolecules* **1973**, *6*, 205.
(18) Matsubayashi, H.; Chatani, Y.; Tadokoro, H.; Dumas, P.; Spassky, N.; Sigwalt, P. *Macromolecules* **1977**, *10*, 996.
(19) Grenier, D.; Prud'homme, R. E. *J. Polym. Sci., Polym. Phys. Ed.* **1984**, *22*, 577.
(20) Lavallée, C.; Prud'homme, R. E. *Macromolecules* **1989**, *22*, 2438.
(21) Ritcey, A. M.; Prud'homme, R. E. *Macromolecules* **1992**, *25*, 972.
(22) Voyer, R.; Prud'homme, R. E. *Eur. Polym. J.* **1989**, *25*, 365.
(23) Ikada, Y.; Jamshidi, K.; Tsuji, H.; Hyon, S.-H. *Macromolecules* **1987**, *20*, 904. This is the first paper of this series.
(24) Tsuji, H.; Horii, F.; Hyon, S.-H.; Ikada, Y. *Macromolecules* **1991**, *24*, 2719.
(25) Tsuji, H.; Hyon, S.-H.; Ikada, Y. *Macromolecules* **1991**, *24*, 5651.
(26) Tsuji, H.; Hyon, S.-H.; Ikada, Y. *Macromolecules* **1991**, *24*, 5657.
(27) Tsuji, H.; Hyon, S.-H.; Ikada, Y. *Macromolecules* **1992**, *25*, 2940.
(28) Tsuji, H.; Ikada, Y. *Macromolecules* **1992**, *25*, 5719.
(29) Tsuji, H.; Horii, F.; Nakagawa, M.; Ikada, Y.; Odani, H.; Kitamaru, R. *Macromolecules* **1992**, *25*, 4114.
(30) Okihara, T.; Tsuji, M.; Kawaguchi, A.; Katayama, K.; Tsuji, H.; Hyon, S.-H.; Ikada, Y. *J. Macromol. Sci., Phys.* **1991**, *B30*, 119.
(31) Okihara, T.; Kawaguchi, A.; Tsuji, H.; Hyon, S.-H.; Ikada, Y.; Katayama, K. *Bull. Inst. Chem. Res. (Kyoto Univ.)* **1988**, *66*, 271.
(32) Shiraki, K.; Tsuji, H.; Hyon, S.-H.; Ikada, Y.; Nakamura, T.; Shimizu, Y. *Polym. Prepr. Jpn.* **1990**, *39*, 584.
(33) Loomis, G. L.; Murdoch, J. R.; Gardner, K. H. *Polym. Prepr. (Am. Chem. Soc., Div. Polym. Chem.)* **1990**, *31* (2), 55.
(34) Yui, N.; Dijkstra, P. J.; Feijen, J. *Makromol. Chem.* **1990**, *191*, 481.
(35) Dijkstra, P. J.; Bulte, A.; Feijen, J. *The 17th Annual Meeting of the Society for Biomaterials*, 1991, p 184.
(36) Hatada, K.; Shimizu, S.; Terawaki, Y.; Ohta, K.; Yuki, H. *Polym. J.* **1981**, *13*, 811.
(37) Sorenson, W. R.; Campbell, T. W., Eds. *Preparative Methods of Polymer Chemistry*; Wiley: New York, 1961.
(38) Hyon, S.-H.; Jamshidi, K.; Ikada, Y. In *Polymers as Biomaterials*; Shalaby, S. W., Hoffman, A. S., Ratner, B. D., Horbett, T. A., Eds.; Plenum Press: New York, London, 1984; pp 51–65.
(39) Schindler, A.; Harper, D. *J. Polym. Sci., Polym. Chem. Ed.* **1979**, *17*, 2593.
(40) Tonelli, A. E.; Flory, P. J. *Macromolecules* **1969**, *2*, 225.
(41) Jamshidi, K.; Hyon, S.-H.; Ikada, Y. *Polymer* **1988**, *29*, 2229.
(42) Schomaker, E.; Challa, G. *Macromolecules* **1988**, *21*, 2195.
(43) Kalb, B.; Pennings, A. J. *Polymer* **1980**, *21*, 607.
(44) Fischer, E. W.; Sterzel, H. J.; Wegner, G. *Kolloid-Z. Z. Polym.* **1973**, *251*, 980.
(45) Vasanthakumari, R.; Pennings, A. J. *Polymer* **1983**, *24*, 175.